The Gray-Scott equations on a bounded domain

Kleinherenbrink, Y.C.

The Gray-Scott equations on a bounded domain

Yvette Kleinherenbrink

August 2007

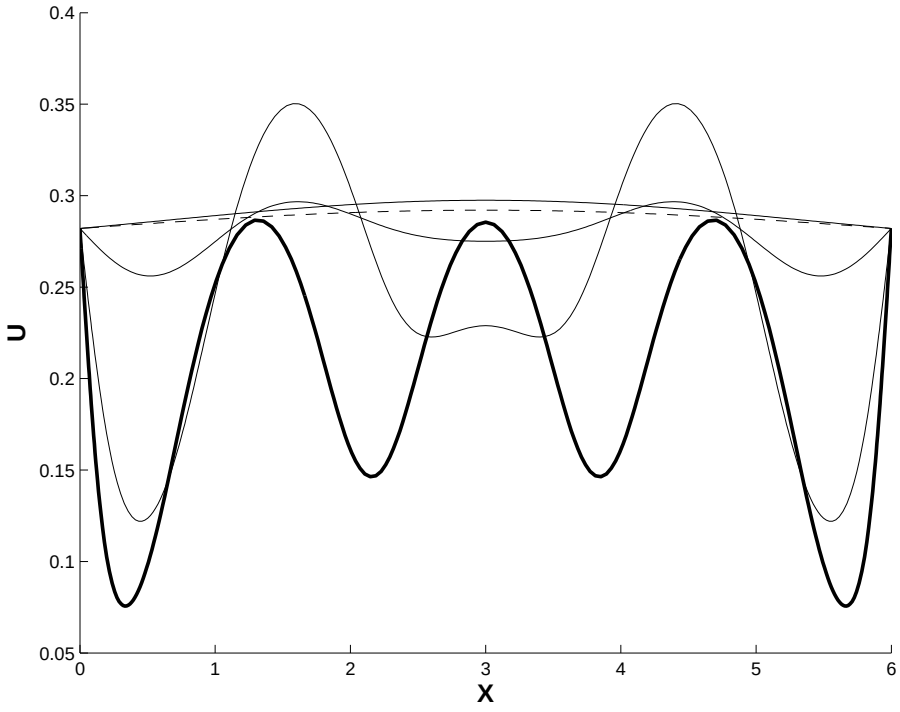

Contents

1 Gray-Scott model

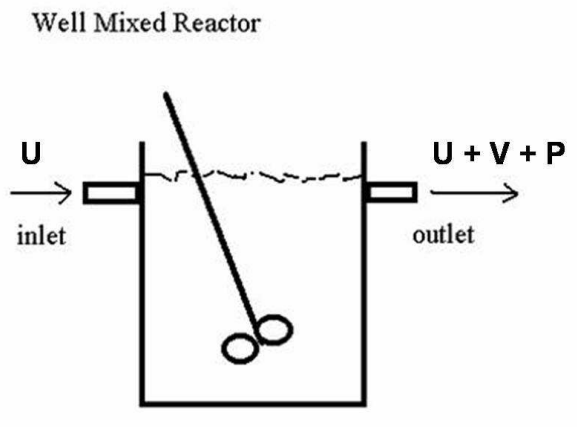

Figure 1: Continuous stirred tank reactor

For the study of a chemical reaction we are going to look at a continuous stirred tank reactor. The reactor contains two chemicals: $\mathcal{U}$ and $\mathcal{V}$. In the tank reactor we have a continuous inlet stream which, in our case, only contains the chemical $\mathcal{U}$ and the product $\mathcal{P}$ is continuously drained. The reactor is well mixed so that there is a uniform concentration of the chemicals $\mathcal{U}$ and $\mathcal{V}$ throughout the reactor.

We study the following chemical reaction: $\mathcal{U} + 2\mathcal{V} \rightarrow 3\mathcal{V}$. This is an autocatalytic reaction in which $\mathcal{V}$ is called the catalyst or the activator and $\mathcal{U}$ the inhibitor of the reaction. Since we want the catalyst $\mathcal{V}$ to have a finite lifetime, we use a second chemical reaction which is of the form $\mathcal{V} \rightarrow \mathcal{P}$.

We introduce the notation $U \equiv U(x,t)$ and $V \equiv V(x,t)$ for the concentrations of the chemical species $\mathcal{U}$ and $\mathcal{V}$, then the equations that model the above situation are given by:

$$\begin{aligned} \frac{\partial U}{\partial t} &= D_U \Delta U - UV^2 + A(1-U) \\ \frac{\partial V}{\partial t} &= D_V \Delta V + UV^2 - BV \end{aligned} \tag{1}$$

These equations were posed by P.Gray and S.K. Scott [2,3] in[1] 1983, that's why it's called the Gray-Scott model.
In this model, the two partial differential equations are the mass-balance equations for $\mathcal{U}$ and $\mathcal{V}$.
In the model D_U and D_V are the diffusivities, which represent the rate of speed by which U en V diffuse. As standard notation, Δ is the Laplacien operator. We are only going to consider the model in one spatial dimension, so that $\Delta U{=}U_{xx}$ and $\Delta V{=}V_{xx}$.

The terms $D_U \Delta U$ and $D_V \Delta V$ in (1) show us how and how fast $\mathcal{U}$ and $\mathcal{V}$ spread themselves in the fluid. To simplify the calculations we choose $D_U = 1$. From now on we write $D_V = D$.

The term UV^2 comes from the fact that one molecule of $\mathcal{U}$ reacts with two molecules of $\mathcal{V}$. In this reaction we lose one $\mathcal{U}$. This leads to a minus sign in the equation of U in front of this term. Since one $\mathcal{V}$ is created in the process, there is a plus sign in the equation of V.
The parameters A and B, $A, B > 0$, represent the rates of the process that feeds U and drains U,V and P. From the assumption that the inlet stream only contains $\mathcal{U}$ we obtain the term A. The terms $-AU$ and $-BV$ are due to the draining.

1.1 The aim of this study

We study the large-time behaviour of solutions $U(x,t)$ and $V(x,t)$ of the Gray-Scott model on a one-dimensional domain where $x \in (0, L)$. We are interested in the parameters A,B and D and the length L of the domain on the profile of a solution as $t \to \infty$; the final profile. To answer the question of which final profile is selected we start by performing numerical simulations. In the simulations, we fix A, B and D and look at the final profile of the solutions as the length of the domain L is varied. We do this for different combinations of A, B and D. Then, we do a linear analysis to take a first step towards explaining the results of the numerical simulations.

2 Stationary states

In a stationary state the solutions U and V don't depend on time, so then $\dfrac{\partial U}{\partial t}$ and $\dfrac{\partial V}{\partial t}$ are equal to zero. Now we look at stationary solutions which are also independent of the spatial variable x. Hence, we take ΔU and ΔV equal to zero. We set

$$\frac{\partial U}{\partial t} = \frac{\partial V}{\partial t} = \Delta U = \Delta V = 0$$

in (1) and get the following equations:

$$\begin{aligned} -UV^2 + A(1-U) &= 0 \qquad (2)\\ UV^2 - BV &= 0. \qquad (3) \end{aligned}$$

We immediately see that the point $(U,V) = (1,0)$ is a solution of the equations (2) and (3). As long as $4B^2 < A$, we obtain two more solutions at

$$(U_\pm, V_\pm) = \left(\frac{1}{2}\left[1 \pm \sqrt{1 - \frac{4B^2}{A}}\right], \frac{A}{2B}\left[1 \mp \sqrt{1 - \frac{4B^2}{A}}\right]\right). \qquad (4)$$

In the case that $4B^2 = A$ these points coincide at $(U,V) = (\frac{1}{2}, 2B)$. This is a special case that not frequently occurs and therefore we do not consider this separately.

3 The model without diffusion

We are interested in the behaviour of the solutions of the Gray-Scott equations (1) as time goes to infinity. To get more insight into system (1), we first study a simpler model. For the reduced model we assume that the concentration of $\mathcal{U}$ and $\mathcal{V}$ don't depend on the spatial variable, i.e. we assume that there is no diffusion. So, ΔU and ΔV are zero and the reduced model becomes:

$$\begin{aligned} \frac{\partial U}{\partial t} &= -UV^2 + A(1-U) \\ \frac{\partial V}{\partial t} &= UV^2 - BV \end{aligned} \tag{5}$$

The three stationary states we found before are the only stationary states of the reduced model.

3.1 Stability

To determine the stability of the stationary states in the reduced model we have to compute the Jacobian matrix of the system. The Jacobian matrix of this system is given by

$$D\mathbf{f}(\mathbf{U},\mathbf{V}) = \begin{pmatrix} -V^2 - A & -2UV \\ V^2 & 2UV - B \end{pmatrix}.$$

For the stationary state $(U,V) = (1,0)$ we find that

$$D\mathbf{f}(\mathbf{1},\mathbf{0}) = \begin{pmatrix} -A & 0 \\ 0 & -B \end{pmatrix}.$$

This matrix has two negative eigenvalues and therefore, the stationary state $(U,V) = (1,0)$ is stable in the model without diffusion.
For the two other stationary states we can determine the eigenvalues of $D\mathbf{f}(\mathbf{U}_{\pm},\mathbf{V}_{\pm})$. Different choices of A and B lead to a charge in character of the stationary state.

3.2 Phaseplane

For certain choices of A and B we plot the two phaseplanes where we plot V versus (see figure 2), by using XPPAUT [6].
In both figures we see that the point $(1,0)$ is stable as also follows from our analysis. The choice of A and B made in figure 2(a) is such that $(1,0)$ is the only fixed point. In figure 2(b) the choice of A and B is such that the solutions (U_{pm}, V_{pm}) do exist. For this choice of A and B, the point (U_-, V_-) is a stable node, whereas (U_+, V_+) is a unstable node.

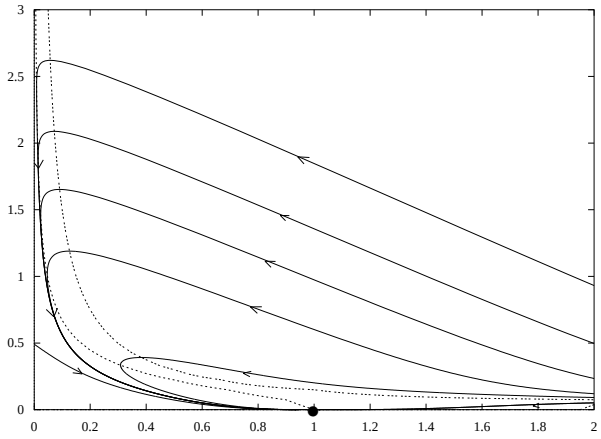

(a) Phaseplane when $4B^2 > A$: $A = 0.05$, $B = 0.15$

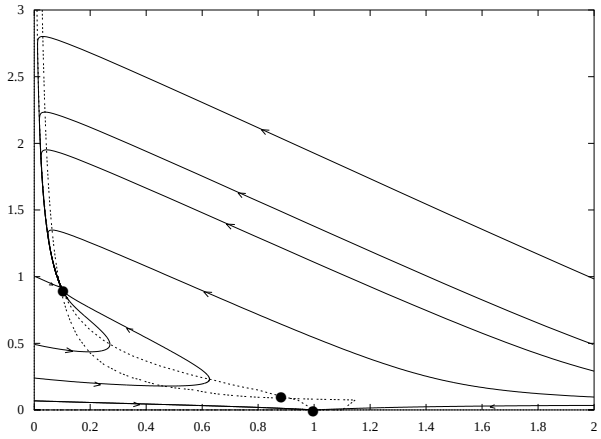

(b) Phaseplane when $4B^2 < A$: $A = 0.09$, $B = 0.086$

Figure 2: Phaseplanes of the reduced model

4 The numerical simulations

For the numerical simulations we use a FORTRAN-code [1] that was given to us by Paul Zegeling (Utrecht). We thank him for letting us use the code and for teaching us how to use it.
In the simulations, we are going to start near a stationary state of the reduced system (5) since several of the stationary states are found to be stable in the reduced case.
In the code we choose the parameters A, B, D and L and we take $x \in [0, L]$. We take D small because experiments and simulations show that it is reasonable to look at the case in which the diffusivity of $\mathcal{U}$ is much larger than that of $\mathcal{V}$. In this case, $\mathcal{U}$ can rapidly go to the regions of high concentration $\mathcal{V}$ so that the reaction will continue. Because we take D small, the regions of high concentration $\mathcal{V}$ remain to exist.

We fix the initial conditions as

$$U(x,0) = U_s + 0.01\sin(\frac{\pi x}{L}) \qquad \text{for} \quad 0 \leq x \leq L$$
$$V(x,0) = V_s - 0.12\sin(\frac{\pi x}{L}) \qquad \text{for} \quad 0 \leq x \leq L$$

where (U_s, V_s) will be chosen to be equal to either (1,0), (U_-, V_-) or (U_+, V_+), see expression (4). The found results of the numerical simulations are independent from the choice of the amplitudes. However, from the linear analysis in section 5 follows that the amplitudes will finally get opposite signs.
Note that it follows from the equations (1) that since these initial functions are symmetric around $x = \frac{1}{2}L$, the solutions $U(x,t)$ and $V(x,t)$ will have the same property for every $t > 0$.

We also have to give the boundary conditions to the code. We used Dirichlet boundary conditions

$$U(0,t) = U_s, \quad U(L,t) = U_s \quad \text{and} \qquad V(0,t) = V_s, \quad V(L,t) = V_s.$$

We are going to look at the solutions $U(x,t)$ and $V(x,t)$ of system (1) numerically as $t \to \infty$ for several choices of A, B, D and L.
In our numerical simulations we only choose $(U_s, V_s) = (U_-, V_-)$, since (U_-, V_-) is stable for our choices of A, B and D. We give the results of the simulations for three different values of A, B and D and we vary L in all cases. The results are given by means of a plot of the initial function, the final solution and a few profiles at intermediate times.

4.1 Numerical Results

4.1.1 Case 1: A = 0.09, B = 0.086, D = 0.01

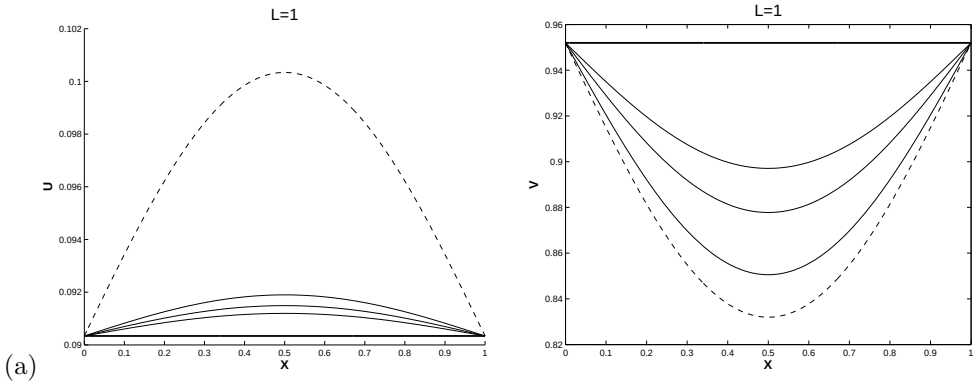

(a)

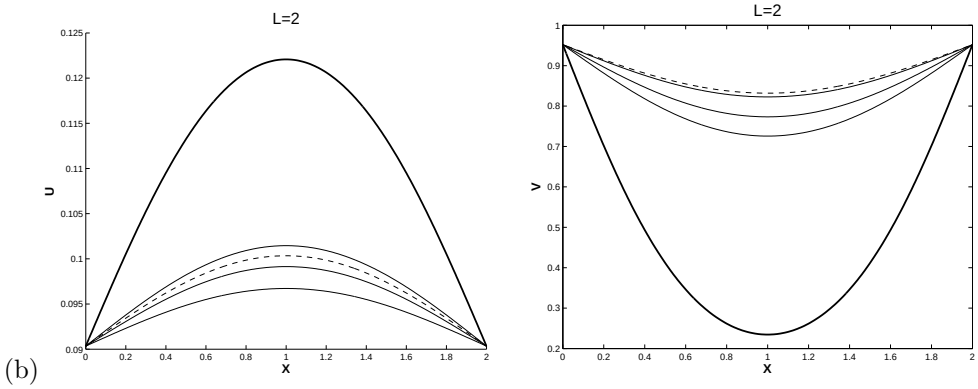

(b)

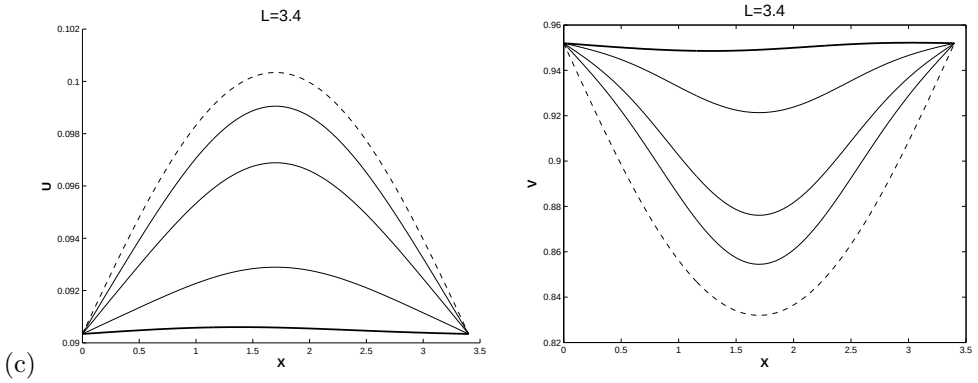

(c)

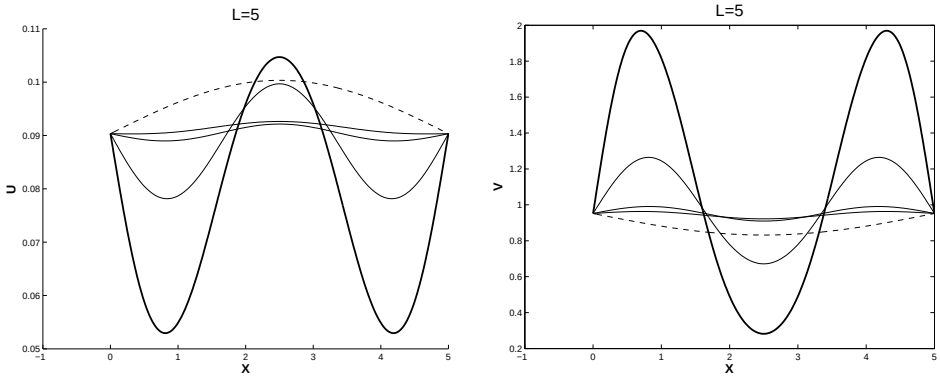

(d)

Figure 3: Solutions for $A = 0.09, B = 0.086$, $D = 0.01$ and (a) $L = 1$, (b) $L = 2$, (c) $L = 3.4$ and (d) $L = 5$. The dashed curve is the initial profile and the thick curve is the final profile. The other curves represent profiles at intermediate times. On the lefthandside the result for U is given and on the righthandside the result for V.

4.1.2 Case 2: A = 1.0, B = 0.45, D = 0.01

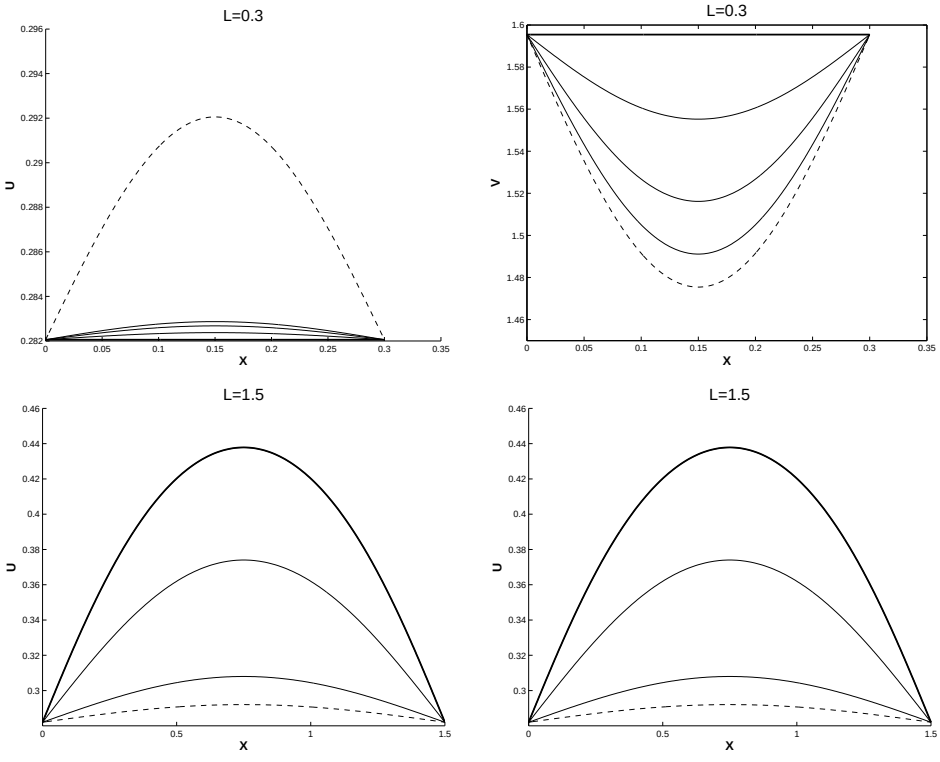

(a)

(b)

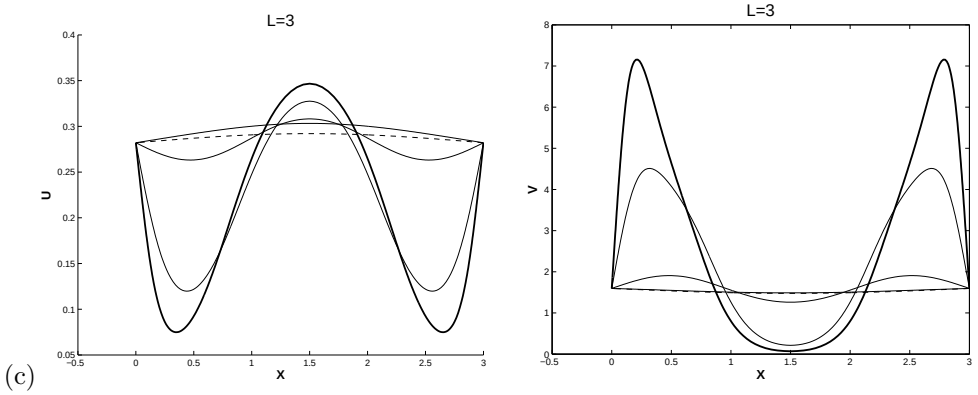

(c)

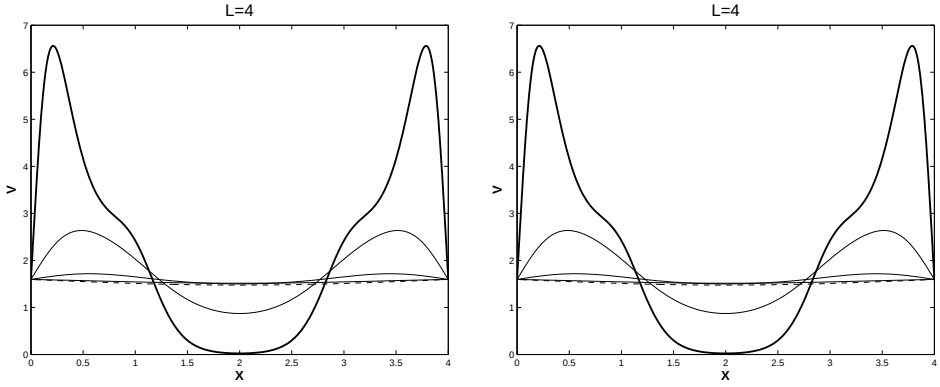

(d)

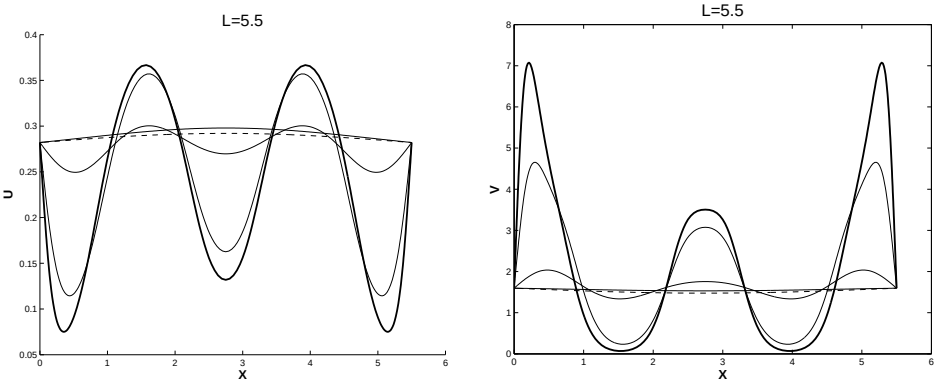

(e)

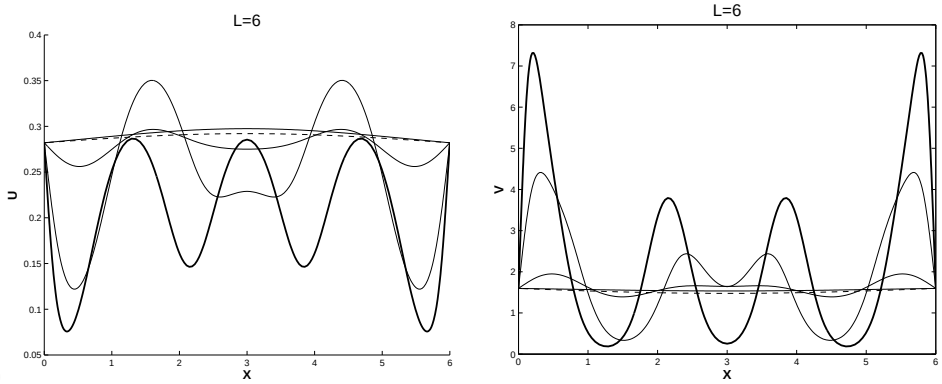

(f)

Figure 4: Solutions for $A = 1.0, B = 0.45$, $D = 0.01$ and (a) $L = 0.3$, (b) $L = 1.5$, (c) $L = 3$, (d) $L = 4$, (e) $L = 5.5$ and (f) $L = 6$. The dashed curve is the initial profile and the thick curve is the final profile. The other curves represent profiles at intermediate times. On the lefthandside the result for U is given and on the righthandside the result for V.

4.1.3 Case 3: A = 0.14, B = 0.1, D = 0.01

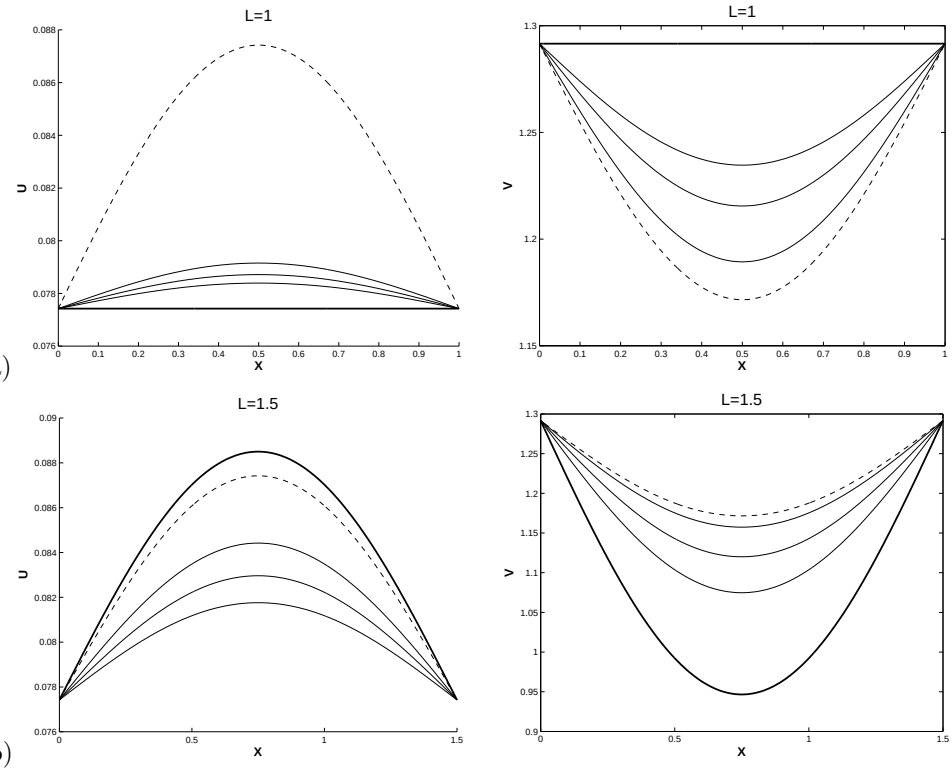

(a)

(b)

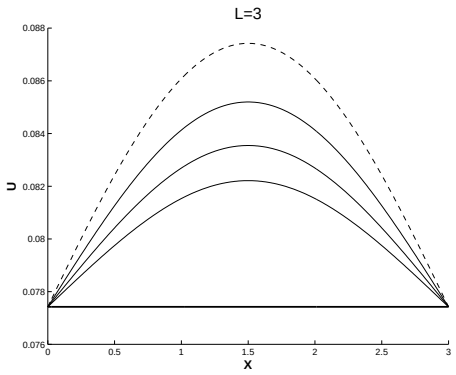

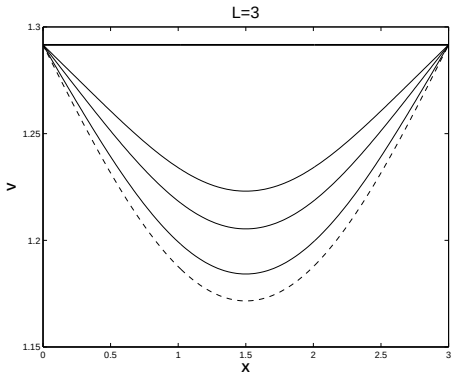

(c)

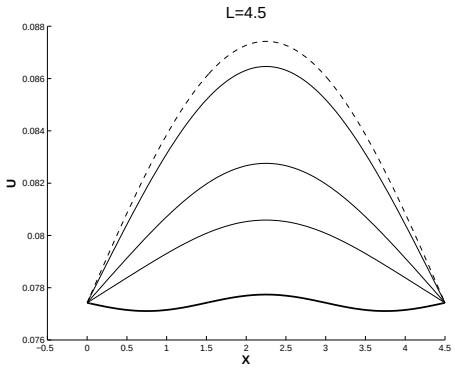

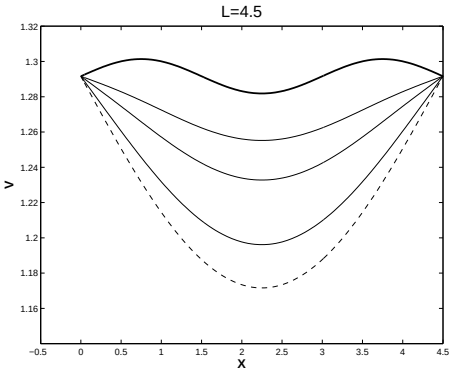

(d)

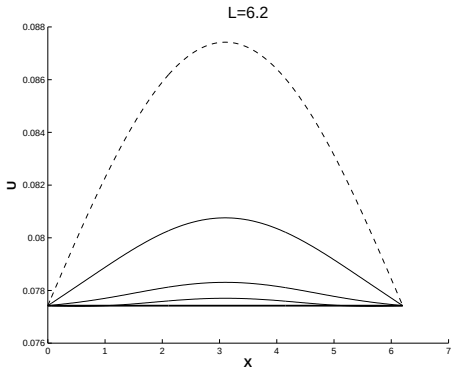

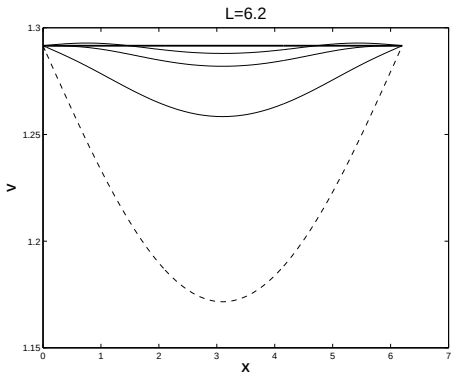

(e)

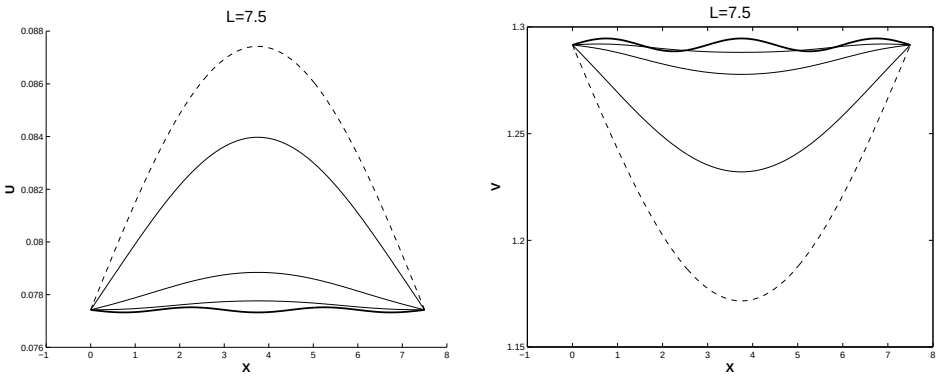

(f)

Figure 5: Solutions for $A = 0.14, B = 0.1$, $D = 0.01$ and (a)$L = 1$, (b) $L = 1.5$, (c) $L = 3$, (d) $L = 4.5$, (e) $L = 6.2$ and (f) $L = 7.5$. The dashed curve is the initial profile and the thick curve is the final profile. The other curves represent profiles at intermediate times. On the lefthandside the result for U is given and on the righthandside the result for V.

4.2 Norm

In figure 3-5 we gave the results of numerical simulations for some values of L. To complete the picture we make a plot of the scaled L^2-norm of the final profiles $u^*(x)$ and $v^*(x)$, see figure 6. Here, we look at the norm with respect to the basic solution (U_s, V_s). We define the L^2-norm of u by

$$\|u\|^2 = \frac{1}{L}\int_0^L (u(x) - U_s)^2 dx,$$

which is rescaled to the interval of lenght L. We do the same for v.

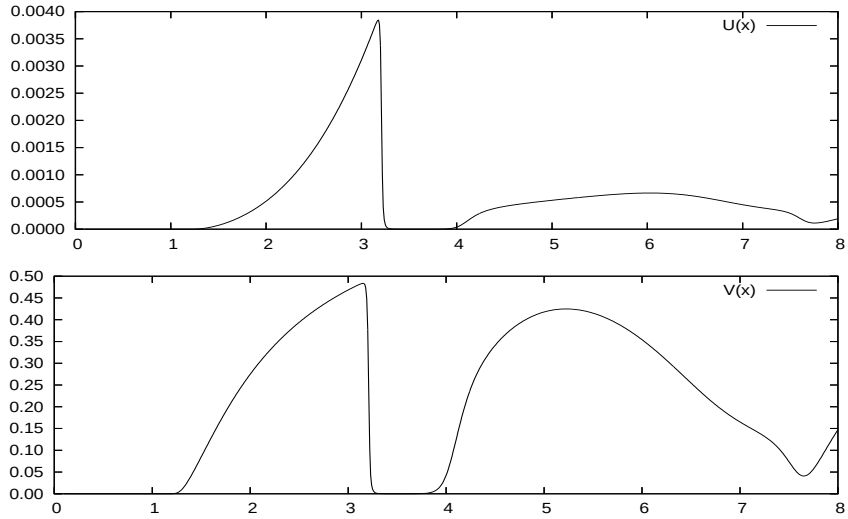

(a) Norm of U(upper) and V(lower) for $A = 0.09$, $B = 0.086$, $D = 0.01$ and $(U_s, V_s) = (U_-, V_-)$

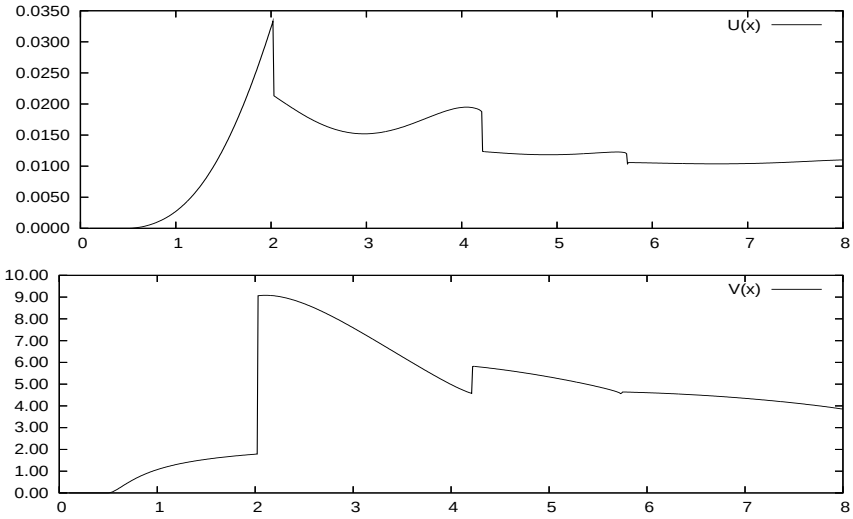

(b) Norm of U(upper) and V(lower) for $A = 1.0$, $B = 0.45$, $D = 0.01$ and $(U_s, V_s) = (U_-, V_-)$

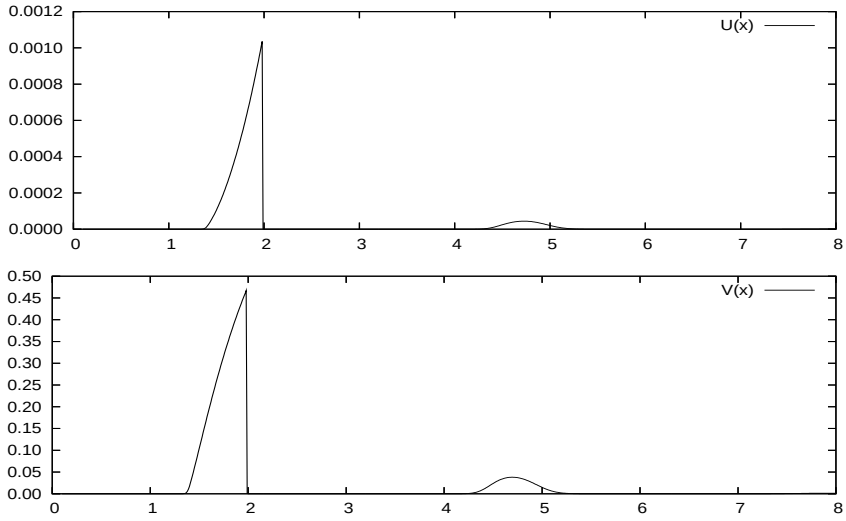

(c) Norm of U(upper) and V(lower) for $A = 0.14$, $B = 0.1$, $D = 0.01$ and $(U_s, V_s) = (U_-, V_-)$

Figure 6: Graphs of the scaled L^2-norm for the three different cases, as L varies.

5 Linear model

As a first step towards understanding the numerical results, we are going to study the linear model. We linearize around the solution (U_s, V_s), where (U_s, V_s) can be taken equal to (U_-, V_-), (U_+, V_+) or $(1, 0)$.
To linearize the model we take $U(x,t) = U_s + \epsilon\tilde{u}(x,t)$ and $V(x,t) = V_s + \epsilon\tilde{v}(x,t)$ where ϵ is small. We substitute this in system (1), leave out all higher order terms of ϵ (since ϵ is small) and omit the tilde. We get the following linear model for the Gray-Scott equations:

$$\begin{aligned} u_t &= u_{xx} - 2Bv - (V_s^2 + A)u \\ v_t &= Dv_{xx} + Bv + V_s^2 u. \end{aligned} \tag{6}$$

The form of this equations gives that we can write the solutions $u(x,t)$ and $v(x,t)$ as a Fourier series:

$$u = \sum_{n=1}^{\infty} a_n w_n(x) e^{-\lambda_n t} \qquad v = \sum_{n=1}^{\infty} b_n z_n(x) e^{-\lambda_n t}.$$

By substituting this into (6) we find the following equations which have to hold

for every $x \in (0, L)$:

$$\begin{aligned} -\lambda_n a_n w_n(x) &= a_n w_n(x)'' - 2B b_n z_n(x) - (V_s^2 + A) a_n w_n(x) \\ -\lambda_n b_n z_n(x) &= D b_n z_n(x)'' + B b_n z_n(x) + V_s^2 a_n w_n(x) \end{aligned} \tag{7}$$

These equations can be solved by substituting

$$\begin{aligned} w_n(x) &= c_{11} \sin(\frac{n\pi x}{L}) + c_{12} \cos(\frac{n\pi x}{L}) \\ z_n(x) &= c_{21} \sin(\frac{n\pi x}{L}) + c_{22} \cos(\frac{n\pi x}{L}). \end{aligned} \tag{8}$$

Since we use Dirichlet boundary conditions we can choose $c_{12} = c_{22} = 0$. We take $c_{11} = c_{21} = \sqrt{2}$ so that w_n and z_n are normalized. If we now substitute (8) in (7), we obtain the following equations:

$$\begin{aligned} -\sqrt{2}\lambda_n a_n \sin(\frac{n\pi x}{L}) &= -\sqrt{2} a_n (\frac{n\pi}{L})^2 \sin(\frac{n\pi x}{L}) - 2\sqrt{2} B b_n \sin(\frac{n\pi x}{L}) \\ &\quad -(V_s^2 + A)\sqrt{2} a_n \sin(\frac{n\pi x}{L}) \\ -\sqrt{2}\lambda_n b_n \sin(\frac{n\pi x}{L}) &= -\sqrt{2} D b_n (\frac{n\pi}{L})^2 \sin(\frac{n\pi x}{L}) + \sqrt{2} B b_n \sin(\frac{n\pi x}{L}) \\ &\quad +\sqrt{2} V_s^2 a_n \sin(\frac{n\pi x}{L}) \end{aligned} \tag{9}$$

We divide by $\sqrt{2}\sin(\frac{n\pi x}{L})$ and write the equations in matrix notation

$$C \cdot \begin{pmatrix} a_n \\ b_n \end{pmatrix} = 0$$

with

$$C = \begin{pmatrix} -\lambda_n + (\frac{n\pi}{L})^2 + V_s^2 + A & 2B \\ -V_s^2 & -\lambda_n + D(\frac{n\pi}{L})^2 - B \end{pmatrix}.$$

The solution $\begin{pmatrix} a_n \\ b_n \end{pmatrix} = \begin{pmatrix} 0 \\ 0 \end{pmatrix}$ satisfies this equation. However, in order to study a perturbation of (U_s, V_s), we want a nontrivial solution for a_n and b_n. We get nontrivial solutions for a_n and b_n if $\det(C) \neq 0$. This implies that

$$\lambda_{n,\pm} = \frac{1}{2}\left(D(\frac{n\pi}{L})^2 - B + (\frac{n\pi}{L})^2 + V_s^2 + A \pm \sqrt{M_n} \right) \tag{10}$$

where

$$M_n = \left(D(\frac{n\pi}{L})^2 - B - (\frac{n\pi}{L})^2 - V_s^2 - A \right)^2 - 8BV_s^2. \tag{11}$$

Note that once A, B, D and n are chosen λ_n is a function of L. Now we are able to plot λ_n versus L for the choices of A, B, D and (U_s, V_s) we made in the numerical simulations, see figure 7.

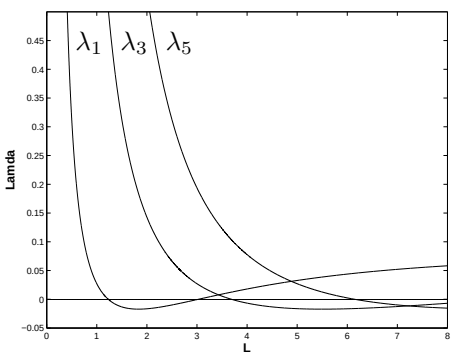

(a) Plot of $\lambda_{n,-}$ for $A = 0.09$, $B = 0.086$, $D = 0.01$ and $(U_s, V_s) = (U_-, V_-)$

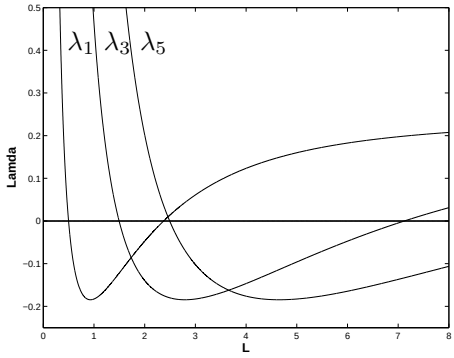

(b) Plot of $\lambda_{n,-}$ for $A = 1.0$, $B = 0.45$, $D = 0.01$ and $(U_s, V_s) = (U_-, V_-)$

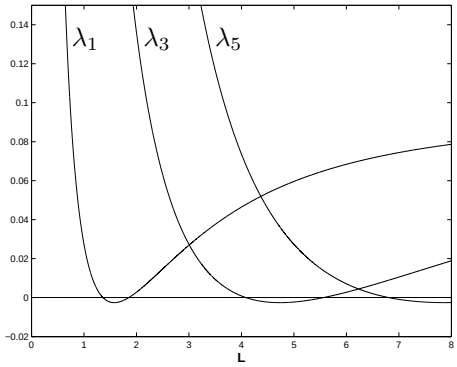

(c) Plot of $\lambda_{n,-}$ for $A = 0.14$, $B = 0.1$, $D = 0.01$ and $(U_s, V_s) = (U_-, V_-)$

Figure 7: Graphs of $\lambda_{n,-}$ against L for the three different cases.

We noted before that $U(x,t)$ and $V(x,t)$ are symmetric for all t, and hence, the final solution will also be symmetric. However, we get an odd function when n is odd. Therefore, we only plotted λ_n for odd n.

In the case that $\lambda_n < 0$ for some $n \in \mathbb{N}$ this leads to instability of the solution (U_s, V_s). When $\lambda_n > 0$ for all $n \in \mathbb{N}$ we expect that the solution will go to the basis solution (U_s, V_s). We are interested in the case when the solution (U_s, V_s) becomes unstable hence whether there exists a λ_n with $\lambda_n < 0$. Therefore, we study the most negative λ_n of the two $\lambda_{n,\pm}$, so $\lambda_{n,-}$, for our further research. Note that we only plotted $\lambda_{n,-}$ in figure 7.

Dividing (9) by $\sin(\frac{n\pi x}{L})$ and substituting $\lambda_{n,-}$, we can express b_n in terms of a_n as follows:

$$b_n = a_n \cdot \frac{\frac{1}{2}\left(D(\frac{n\pi}{L})^2 - B - (\frac{n\pi}{L})^2 - V_s^2 - A - \sqrt{M_n}\right)}{2B} \tag{12}$$

6 Relation between the numerical results and the linear analysis

In this section we try to explain the numerical results for the three different cases using the linear analysis of section 5.
Let L_1 and L_2 ($L_1 < L_2$) be the zero's of λ_1. Because of the relation between λ_n and λ_1, the points nL_1 and nL_2 are the zero's of λ_n (see chapter 5).

6.1 Case 1: A = 0.09, B = 0.086, D = 0.01

For $L < L_1 \approx 1.23$, for example when $L = 1$, the solutions seem to go to the solution (U_-, V_-), see figure 3(a). When $L_1 < L < L_2 \approx 3.03$ we see in figure 6(a) that there is a branch of solutions which bifurcates off the basis solution (U_-, V_-) close to $L \approx L_1 \approx 1.23$ and returns again near $L \approx L_2 \approx 3.03$. We see this in figure 3(b) for $L = 2$ and for this value of L the limiting solution of U and V looks like a $\frac{1}{2}\sin(x)$. For $L_2 < L < 3L_1 \approx 3.69$ the solution seem to go to the solution (U_-, V_-) again, for example for $L = 3.4$; see figure 3(c). At $L \approx 3L_1$, we see that there is a new branch that bifurcates. For example, when $L = 5$ we find that the limited solution looks like $a\sin(x) + b\sin(3x)$ for some values of a and b; see figure 3(d).

6.2 Case 2: A = 1.0, B = 0.45, D = 0.01

For this case we see that the final solution is only going to (U_-, V_-) for
$L < L_1 \approx 0.50$. In figure 4(a) the result is shown for $L = 0.3$. In figure 6(b) we see that a branch bifurcates at $L \approx L_1$. We see several nontrivial final states as shown in figure 4(b)-4(f) for $L = 1.5$, $L = 3$, $L = 4$, $L = 5.5$ and $L = 6$. We see that all of the final solutions are a combination of $\sin(nx)$ for several values of n. In figure 6(b) we also see some discontinuities when $L > L_1$. So far, we do not have an explanation for this phenomenon.

6.3 Case 3: A = 0.14, B = 0.1, D = 0.01

In figure 6(c) we see that for $1.36 \approx L_1 < L < L_2 \approx 1.85$ and for
$4.09 \approx 3L_1 < L < 3L_2 \approx 5.56$ there is a branch that bifurcates off the basis solution (U_-, V_-). For the other values of L the solution seem to go to the basis solution (U_-, V_-). In figure 5(a)- 5(f) the results are shown for $L = 1$, $L = 1.5$, $L = 3$, $L = 4.5$, $L = 6.2$ and $L = 7.5$.

7 Local behaviour around L_1

In this section we study the bifurcations off the solutions (U_s, V_s) that we saw in figure 6. We derive equations for the norms $\|u\|$ and $\|v\|$ in the neighbourhood of the bifurcation points L_1 and L_2.
It will be convenient to scale the variable x to a fixed interval [0,1]. Thus, we introduce the variables $\tilde{x}$, $\tilde{u}$ and $\tilde{v}$:

$$x = L\tilde{x}, \qquad U(x,t) = U_s + \tilde{u}(\tilde{x},t) \quad \text{and} \quad V(x,t) = V_s + \tilde{v}(\tilde{x},t).$$

From now on we drop the tilde again. In terms of the new variables a stationary solution will be a solution of the following problem:

$$\mathcal{L}(u,v,L) + \begin{pmatrix} L^2(-U_s v^2 - 2V_s uv - uv^2) \\ L^2(U_s v^2 + 2V_s uv + uv^2) \end{pmatrix} = 0 \tag{13}$$

where

$$\mathcal{L}(u,v,L) = \begin{pmatrix} \mathcal{L}_1(u,v,L) \\ \mathcal{L}_2(u,v,L) \end{pmatrix} = \begin{pmatrix} u_{xx} - L^2(2Bv + V_s^2 u + Au) \\ Dv_{xx} + L^2(Bv + V_s^2 u) \end{pmatrix}$$

which is the linear system (6) that we studied in section 5.
From our linear analysis it follows that the eigenfunctions of the eigenvalue problem for the linear operator $\mathcal{L}$ are given by

$$\Psi_n = \begin{pmatrix} \psi_n \\ c\psi_n \end{pmatrix}$$

where $\psi_n = \sqrt{2}\sin(n\pi x)$ and $c_n = \dfrac{b_n}{a_n} = \dfrac{\frac{1}{2}\left(D(\frac{\pi}{L})^2 - B - (\frac{\pi}{L})^2 - V_s^2 - A - \sqrt{M_n}\right)}{2B}$

and M_n is given by expression (11).
We are going to focus on the bifurcation at $L = L_1$, where L_1 is the smallest solution for which $\lambda_1 = 0$, hence, $n = 1$ in the above expression. Since we want to study the relation between u, v and L near the point $(L,u,v) = (L_1, 0, 0)$ we write

$$L = L_1(1+\xi), \quad u = \epsilon(\psi_1 + y_1) \quad \text{and} \quad v = \epsilon(c_1\psi_1 + y_2),$$

where ϵ, ξ, y_1 and y_2 are small. Substitution in equation (13) gives us the following equation:

$$\mathcal{L}(y_1, y_2, L_1) = h(y_1, y_2, \xi, \epsilon) = \begin{pmatrix} h_1(y_1, y_2, \xi, \epsilon) \\ h_2(y_1, y_2, \xi, \epsilon) \end{pmatrix} \tag{14}$$

where

$$\begin{aligned} h_1(y_1,y_2,\xi,\epsilon) &= L_1^2\left\{(1+\xi)^2-1\right\}\left[2B(c_1\psi_1+y_2)+(V_s^2+A)(\psi_1+y_1)\right] \\ &\quad +L_1^2(1+\xi)^2\left[U_s\epsilon(c_1\psi_1+y_2)^2+2V_s\epsilon(\psi_1+y_1)(c_1\psi_1+y_2)\right. \\ &\quad \left.+\epsilon^2(\psi_1+y_1)(c_1\psi_1+y_2)^2\right] \end{aligned}$$

$$\begin{aligned} h_2(y_1,y_2,\xi,\epsilon) &= -L_1^2\left\{(1+\xi)^2-1\right\}\left[B(c_1\psi_1+y_2)+V_s^2(\psi_1+y_1)\right] \\ &\quad -L_1^2(1+\xi)^2\left[U_s\epsilon(c_1\psi_1+y_2)^2+2V_s\epsilon(\psi_1+y_1)(c_1\psi_1+y_2)\right. \\ &\quad \left.+\epsilon^2(\psi_1+y_1)(c_1\psi_1+y_2)^2\right] \end{aligned}$$

Now we use Lin's method [4,5]. We introduce the subspaces X_0 and X_1 of $X = L^2(\Omega)$ defined by

$$X_0 = \{s\Psi_1 : s \in \mathrm{R}\} \quad \text{and} \quad X_1 = \{z \in \mathrm{R}^2 : (z,\Psi_1) = 0\},$$

and we denote the orthogonal projection of X onto X_0 by $\mathcal{P}$. We then first solve the problem

$$\mathcal{L}(y_1,y_2,L_1) = (\mathcal{I}-\mathcal{P})h(y_1,y_2,\xi,\epsilon) \quad \text{for} \quad x \in (0,1), \quad y_1,y_2 = 0 \quad \text{at} \quad x = 0,1. \tag{15}$$

The right-hand side in (15) is an element of X_1, and the operator $\mathcal{L}(\cdot;\cdot;L_1)$ is nonsingular on X_1. By a contraction argument one can show that for some small constant $\rho > 0$ there exist unique solutions $y_1^*(\xi,\epsilon)$ and $y_2^*(\xi,\epsilon)$ of problem (15) as long as $|\xi| < \rho$, $|\epsilon| < \rho$, $\|y_1\| < \rho$ and $\|y_2\| < \rho$, such that $y_1^*(0,0) = y_2^*(0,0) = 0$. These solutions will be solutions of the original equation (14) if

$$\mathcal{P}h(y_1^(\xi,\epsilon), y_2^*(\xi,\epsilon),\xi,\epsilon) = 0,$$

which means that

$$\begin{aligned} \mathcal{G}(\xi,\epsilon) &= \int_0^1 \Psi_1 \bullet h(y_1^*(\xi,\epsilon),y_2^*(\xi,\epsilon),\xi,\epsilon)dx \\ &= \int_0^1 \psi_1 h_1(y_1^*(\xi,\epsilon),y_2^*(\xi,\epsilon),\xi,\epsilon)dx + \int_0^1 c_1\psi_1 h_2(y_1^*(\xi,\epsilon),y_2^*(\xi,\epsilon),\xi,\epsilon)dx \\ &= \mathcal{G}_1(\xi,\epsilon)+\mathcal{G}_2(\xi,\epsilon) = 0. \end{aligned}$$

By standard ODE theory, y_1^* and y_2^* are smooth functions of ξ and ϵ, and hence $\mathcal{G}$ is also a smooth function of ξ and ϵ. Thus, by applying the Implicit Function Theorem, we find that if $\mathcal{G}(0,0) \neq 0$, then ξ is a differentiable function of ϵ, and

$$\mathcal{G}_{1,\xi}\frac{d\xi}{d\epsilon} + \mathcal{G}_{1,\epsilon} + \mathcal{G}_{2,\xi}\frac{d\xi}{d\epsilon} + \mathcal{G}_{2,\epsilon} = 0,$$

so that

$$\frac{d\xi}{d\epsilon} = -\frac{\mathcal{G}_{1,\epsilon}+\mathcal{G}_{2,\epsilon}}{\mathcal{G}_{1,\xi}+\mathcal{G}_{2,\xi}},$$

where $\mathcal{G}_{1,\xi}, \mathcal{G}_{1,\epsilon}, \mathcal{G}_{2,\xi}$ and $\mathcal{G}_{2,\epsilon}$ have to be computed in the origin.

Calculations show that

$$h_1(0,0,0,0) = 0, \quad h_2(0,0,0,0) = 0, \quad h_{1,y_1}(0,0,0,0) = 0, \quad h_{2,y_1}(0,0,0,0) = 0$$

$$h_{1,y_2}(0,0,0,0) = 0, \quad h_{2,y_2}(0,0,0,0) = 0,$$

$$h_{1,\xi}(0,0,0,0) = 4L_1^2 B c_1 \psi_1 + 2L_1^2(V_s^2 + A)\psi_1,$$

$$h_{2,\xi}(0,0,0,0) = -2L_1^2 V_s^2 \psi_1 - 2L_1^2 B c_1 \psi_1.$$

Thus,

$$\begin{aligned}
\mathcal{G}_{1,\epsilon}(0,0) &= L_1^2 \int_0^1 U_s c_1^2 \psi_1^3 + 2V_s c_1 \psi_1^3 dx = L_1^2(2\sqrt{2}U_s c_1^2 + 4\sqrt{2}V_s c_1)\frac{4}{3\pi} \\
\mathcal{G}_{2,\epsilon}(0,0) &= L_1^2 \int_0^1 -U_s c_1^3 \psi_1^3 - 2V_s c_1^2 \psi_1^3 dx = L_1^2(-2\sqrt{2}U_s c_1^3 - 4\sqrt{2}V_s c_1^2)\frac{4}{3\pi} \\
\mathcal{G}_{1,\xi}(0,0) &= 2L_1^2 \int_0^1 2Bc_1\psi_1^2 + (V_s^2 + A)\psi_1^2 dx = 2L_1^2(2Bc_1 + V_s^2 + A) \\
\mathcal{G}_{2,\xi}(0,0) &= 2L_1^2 \int_0^1 -V_s^2 c_1 \psi_1^2 - Bc_1^2 \psi_1^2 dx = 2L_1^2(-V_s^2 c_1 - Bc_1^2)
\end{aligned}$$

So we find that

$$\frac{d\xi}{d\epsilon} = -\frac{2}{3\pi} \cdot \frac{2\sqrt{2}U_s c_1^2(1-c_1) + 4\sqrt{2}V_s c_1(1-c_1)}{Bc(2-c_1) + V_s^2(1-c_1) + A}.$$

From this we conclude that

$$\xi = -\frac{2\epsilon}{3\pi} \cdot \frac{2\sqrt{2}U_s c_1^2(1-c_1) + 4\sqrt{2}V_s c_1(1-c_1)}{Bc(2-c_1) + V_s^2(1-c_1) + A} + \text{h.o.t.}$$

Also,

$$\int_0^1 u^2 dx = \epsilon^2 \int_0^1 \psi_1^2 dx + \text{h.o.t} = \epsilon^2 + \text{h.o.t} \quad \text{and}$$

$$\int_0^1 v^2 dx = c_1^2 \epsilon^2 \int_0^1 \psi_1^2 dx + \text{h.o.t} = c_1^2 \epsilon^2 + \text{h.o.t.}$$

Now, we use that

$$\xi = \frac{L - L_1}{L_1},$$

to find that

$$\int_0^1 u^2 dx \sim \epsilon^2 \sim \frac{9\pi^2}{4L_1^2} \cdot \frac{\big(Bc_1(2-c_1) + V_s^2(1-c_1) + A\big)^2}{\big(2\sqrt{2}U_s c_1^2(1-c_1) + 4\sqrt{2}V_s c_1(1-c_1)\big)^2} \cdot (L - L_1)^2 \quad \text{as} \quad L \searrow L_1$$

and

$$\int_0^1 v^2 dx \sim c_1\epsilon^2 \sim \frac{9c_1^2\pi^2}{4L_1^2}\cdot\frac{\left(Bc_1(2-c_1)+V_s^2(1-c_1)+A\right)^2}{\left(2\sqrt{2}U_s c_1^2(1-c_1)+4\sqrt{2}V_s c_1(1-c_1)\right)^2}\cdot(L-L_1)^2 \quad \text{as} \quad L\searrow L_1.$$

If we return to the original variables, and using that

$$\|u\|^2 = \frac{1}{L}\int_0^1 (U-U_s)dx = \int_0^1 \tilde{u}^2 d\tilde{x} \quad \text{and} \quad \|v\|^2 = \tfrac{1}{L}\int_0^1 (V-V_s)dx = \int_0^1 \tilde{v}^2 d\tilde{x},$$

we get that

$$\|u\|^2 \sim \frac{9\pi^2}{4L_1^2}\cdot\frac{\left(Bc_1(2-c_1)+V_s^2(1-c_1)+A\right)^2}{\left(2\sqrt{2}U_s c_1^2(1-c_1)+4\sqrt{2}V_s c_1(1-c_1)\right)^2}\cdot(L-L_1)^2 \quad \text{as} \quad L\searrow L_1$$

and

$$\|v\|^2 \sim \frac{9\pi^2 c_1^2}{4L_1^2}\cdot\frac{\left(Bc_1(2-c_1)+V_s^2(1-c_1)+A\right)^2}{\left(2\sqrt{2}U_s c_1^2(1-c_1)+4\sqrt{2}V_s c_1(1-c_1)\right)^2}\cdot(L-L_1)^2 \quad \text{as} \quad L\searrow L_1.$$

If we replace L_1 by L_2 in the above expressions, we obtain the norms around the bifurcation point $L = L_2$.
If we compute the coefficient of $(L-L_1)^2$ in above expressions for the three different cases, we get the following:

Case 1:
$$\begin{aligned}
\|u\|^2 &\sim 4.73\cdot 10^{-6}\cdot(L-L_1)^2 \quad \text{as} \quad L\searrow L_1\\
\|v\|^2 &\sim 0.0091\cdot(L-L_1)^2 \quad \text{as} \quad L\searrow L_1\\
\|u\|^2 &\sim 8.28\cdot 10^{-7}\cdot(L-L_2)^2 \quad \text{as} \quad L\searrow L_2\\
\|v\|^2 &\sim 1.20\cdot 10^{-4}\cdot(L-L_2)^2 \quad \text{as} \quad L\searrow L_2
\end{aligned}$$

Case 2:
$$\begin{aligned}
\|u\|^2 &\sim 9.14\cdot 10^{-4}\cdot(L-L_1)^2 \quad \text{as} \quad L\searrow L_1\\
\|v\|^2 &\sim 2.1095\cdot(L-L_1)^2 \quad \text{as} \quad L\searrow L_1\\
\|u\|^2 &\sim 2.30\cdot 10^{-4}\cdot(L-L_2)^2 \quad \text{as} \quad L\searrow L_2\\
\|v\|^2 &\sim 0.0080\cdot(L-L_2)^2 \quad \text{as} \quad L\searrow L_2
\end{aligned}$$

Case 3:
$$\begin{aligned}
\|u\|^2 &\sim 4.26\cdot 10^{-6}\cdot(L-L_1)^2 \quad \text{as} \quad L\searrow L_1\\
\|v\|^2 &\sim 0.0054\cdot(L-L_1)^2 \quad \text{as} \quad L\searrow L_1\\
\|u\|^2 &\sim 1.98\cdot 10^{-6}\cdot(L-L_2)^2 \quad \text{as} \quad L\searrow L_2\\
\|v\|^2 &\sim 0.0011\cdot(L-L_2)^2 \quad \text{as} \quad L\searrow L_2
\end{aligned}$$

8 Conclusion

In this study we considered the large-time behaviour of solutions $U(x,t)$ and $V(x,t)$ of the Gray-Scott model on a one-dimensional domain $(0,L)$. We focused on the parameters A, B and D and on the length L of the domain. We did look at the final profiles of the model for three different values of A, B and D by doing some numerical simulations. With some linear analysis we tried to explain the behaviour which we saw in our numerical results. It appears that for some values of A, B and D and for small L, we can give a nice explanation of our numerical results using the linear model. We also did a bifurcation analysis of nontrivial solutions branching off the basis solution (U_s, V_s).

9 References

1. J.G. Blom, P.A. Zegeling, 1994. Algorithm 731: A moving-grid interface for systems of one-dimensional time-dependent partial differential equations. *ACM Transactions on Mathematical Software* 20, 194-214.

2. P. Gray, S.K. Scott, 1983. Autocatalytic reactions in the isothermal, continuous stirred tank reactor: isolas and other forms of multistability. *Chem. Eng. Sci.* 38, 29-43.

3. P. Gray, S.K. Scott, 1984. Autocatalytic reactions in the isothermal, continuous stirred tank reactor: oscillations and instabilities in the system $A + 2B \rightarrow 3B$, $B \rightarrow C$. *Chem. Eng. Sci.* 39, 1087-1097.

4. J.K. Hale, L.A. Peletier, W.C. Troy, 2000. Exact homoclinic and heteroclinic solutions of the Gray-Scott model for autocatalysis. *SIAM J. Appl. Math.* Vol. 61, No. 1, 102-130.

5. X.-B. Lin, 1990. Using Mel'nikov's method to solve Sil'nikov's problems. *Proc. R. Soc. Edinburgh A* 116, 295-325

6. Bard Ermentrout, 2002. XPPAUT 5.9 Copyright.